Frontiers in Bioscience Landmark

Front. Biosci. (Landmark Ed) **2026**; 31(8): 52014
https://doi.org/10.31083/FBL52014

Original Research

Experimental Study on Anti-Infection and Promotion of Macrophage Polarization for the Treatment of Traumatic Bone Infection Using Rifampicin/Moxifloxacin-Loaded PLGA Microspheres

Jing An[1], Yafeng Zhang[2,3], Peijie Zhao[2,3], Tao Ding[2,3], Huanhuan Sun[2,3], Zhipeng Yang[2,3], Huanxiang Guan[2,3], Yaodong Wang[2,3], Hairui Fang[2,3], Zewen Qiao[3,*]

[1]Department of Pharmacy, Peking University First Hospital, Ningxia Women and Children Hospital, 750000 Yinchuan, Ningxia, China
[2]The First Clinical Medical College of Ningxia Medical University, 750000 Yinchuan, Ningxia, China
[3]Orthopedic Department of Hands, Feet and Ankles, Ningxia Medical University General Hospital, 750000 Yinchuan, Ningxia, China
*Correspondence: 13995307859@163.com (Zewen Qiao)
Academic Editor: Elisa Belluzzi
Submitted: 18 March 2026 Revised: 18 June 2026 Accepted: 22 June 2026 Published: 21 August 2026

Abstract

Background: Traumatic osteomyelitis remains a prevalent and intractable clinical disorder in orthopedics. Treatment of this condition is severely hindered by multiple factors, including multidrug-resistant bacterial infections (predominantly methicillin-resistant Staphylococcus aureus, MRSA), the blood-bone barrier, infection-induced bone necrosis, and the internalization capacity of bone cells. Current therapeutic strategies mainly consist of debridement, systemic antibiotic administration, and local sustained-release antibiotic delivery. Local biodegradable materials with sustained antibiotic release may help maintain effective antibacterial exposure at infectious sites and may be associated with favorable changes in the inflammatory microenvironment during infection resolution and tissue repair. **Materials and Methods:** Our research team has previously constructed rifampicin/moxifloxacin-loaded Poly(lactic-co-glycolic acid) (PLGA) sustained-release microspheres and validated their favorable sustained-release characteristics and antibacterial properties *in vitro*. In the present study, we further investigated their therapeutic efficacy against traumatic osteomyelitis, with a focus on infection-related pathological changes and macrophage polarization-associated inflammatory responses. A murine femoral traumatic osteomyelitis model was established, and animals were assigned to three groups (control, model, and rifampicin–moxifloxacin (RM)-PLGA treatment) for comparative intervention. General observation, X-ray examination, and histopathological staining were performed for evaluation. Additionally, serological analysis, histopathological assessment, western blotting, and immunofluorescence were used to detect relevant indicators. *In vitro* experiments using infected RAW264.7 macrophages co-cultured with microspheres were conducted to further verify the effects. **Results:** General observation, X-ray examination, and histopathological staining revealed that local infection was markedly alleviated in the microsphere group, whereas persistent infection-related changes were observed in the model group, and the control group remained largely normal. Serological analysis, histopathological assessment, Western blot, and immunofluorescence showed that RM-PLGA treatment attenuated inflammatory responses and was associated with changes in macrophage polarization-associated markers. *In vitro*, RM-PLGA treatment reduced IL-6 and IL-1β levels, increased IL-10 levels, and significantly decreased the fluorescence intensities of both CD38 and CD206. *In vivo*, RM-PLGA treatment reduced serum pro-inflammatory cytokine levels and CD38 fluorescence intensity. CD206 fluorescence intensity was comparable to that in the model group on day 7 but was significantly lower on days 14 and 28; serum IL-10 levels were significantly lower on days 7 and 28 and did not differ significantly on day 14. In addition, RM-PLGA treatment was accompanied by changes in the expression of YTHDC1, PDPK1, and PTGS2, suggesting that these molecules may be associated with infection resolution and inflammatory microenvironment remodeling. However, further functional validation is required to confirm their causal roles. **Conclusion:** Collectively, these findings suggest that rifampicin/moxifloxacin-loaded PLGA microspheres may represent a promising local therapeutic strategy for traumatic osteomyelitis by alleviating infection-related pathological changes and promoting favorable changes in macrophage polarization markers.

Keywords: osteomyelitis; bacterial infections; antibacterial agents; macrophage polarization-associated markers; RM-PLGA microspheres

1. Introduction

Traumatic osteomyelitis is currently one of the most common bone infectious diseases in clinical practice [1]. Approximately 5–30% of severe open fractures develop into traumatic osteomyelitis, whereas implant surgeries are associated with infection rates of approximately 2–5% [2,3]. In clinical practice, patients with traumatic osteomyelitis face challenges such as multiple surgeries, prolonged treatment courses, high recurrence rates, and poor prognosis, thereby imposing significant mental and economic burdens on patients, doctors, and society [4,5,6].

The complete cure of traumatic osteomyelitis is highly challenging [7]. Repeated debridement and systemic application of antibiotics do not effectively shorten the treatment course or reduce recurrence [8,9,10]. Local bone and soft-tissue injuries caused by trauma provide an environment more susceptible to bacterial invasion and rapid spread to surrounding areas [11,12]. Ischemia in the lesion area and the presence of the blood-bone barrier make it difficult for intravenously administered antibiotics to reach bactericidal concentrations [9,10]. Low concentrations of antibiotics at the infection site are ineffective and prone to inducing bacterial resistance, while increasing antibiotic concentrations further exacerbates adverse drug reactions [13]. Studies show that 75% of traumatic osteomyelitis is caused by Staphylococcus aureus [14,15]. *S. aureus* can evade host immune responses and antibiotic-mediated killing by forming biofilms and intracellular internalization [14]. Biofilms are microenvironments composed of extracellular matrix and bacteria formed within hours of bacterial invasion, enhancing bacterial defense capabilities and providing nutrients for their proliferation and spread [16,17]. Additionally, Staphylococcus aureus can invade non-professional phagocytic cells such as osteoblasts, fibroblasts, and endothelial cells [18]. Internalized bacteria can evade immune responses and kill host cells by disrupting cell membranes, leading to tissue necrosis [19,20]. Necrotic bone tissue can then serve as an attachment site for bacteria, perpetuating new infections [21]. Therefore, in addition to thorough surgical debridement, current research focuses on how to increase antibiotic concentration and bactericidal efficiency in the lesion area while restoring the immune microenvironment to promote tissue regeneration [9,22].

Local sustained-release antibiotic therapy for osteomyelitis is designed to increase antibiotic exposure at the lesion site and reduce systemic toxicity. Poly(lactic-co-glycolic acid) (PLGA) is a biodegradable high-molecular-weight organic compound composed of lactic acid (LA) and glycolic acid (GA). After entering the body, PLGA undergoes ester bond hydrolysis to generate corresponding lactic acid, glycolic acid, and monomeric acids, which are then converted into water and carbon dioxide via the tricarboxylic acid cycle [9,23]. Therefore, PLGA offers advantages such as low immunogenicity, good biocompatibility, and controllable biodegradability, making it a key research focus as a sustained-release carrier for drugs, proteins, peptides, and even genes [24]. PLGA has also been extensively studied as an antibiotic carrier for osteomyelitis treatment. Gatifloxacin-PLGA composite with β-tricalcium phosphate has demonstrated antibacterial activity against Streptococcus milleri and Bacteroides fragilis in clinical settings. *In vivo* animal experiments have found that this composite can inhibit inflammatory responses and exert therapeutic effects on osteomyelitis animal models [25,26,27].

Rifampicin and moxifloxacin are highly effective broad-spectrum antibiotics that are characterized by high bioavailability in bone and good penetration of biofilms [13,20,28]. Studies have shown that the combined application of rifampicin and moxifloxacin significantly improves the cure rate of osteomyelitis and reduces the occurrence of drug resistance, making them widely used in treating bone infections [12]. Recent research has suggested that rifampicin and moxifloxacin may be associated with changes in macrophage polarization-related inflammatory responses during bacterial clearance and tissue repair. PTGS2-related pathways may be involved in this process, although direct causal evidence remains limited [29,30].

In our previous study, rifampicin/moxifloxacin-loaded PLGA microspheres were successfully prepared using a water-in-oil-in-water double emulsion solvent evaporation technique. These microspheres showed favorable morphology, sustained drug-release behavior, and improved encapsulation efficiency. More importantly, their direct *in vitro* antibacterial and anti-biofilm activities against Staphylococcus aureus were systematically confirmed by time-kill assays, Kirby–Bauer inhibition-zone tests, crystal violet biofilm quantification, and confocal laser scanning microscopy. Rifampicin (RIF)/moxifloxacin (MOX)–PLGA microspheres demonstrated stronger antibacterial activity and biofilm-inhibition capacity than MOX–PLGA or blank PLGA microspheres [31]. Based on these previous findings, the present study further investigated the *in vivo* therapeutic efficacy of RIF/MOX–PLGA microspheres in a traumatic osteomyelitis model, with particular emphasis on infection-related pathological outcomes and macrophage polarization.

2. Materials and Methods

2.1 Materials

PLGA (LA/GA = 50/50, MW = 9×10^4 Da) was purchased from Shandong Medical Instrument Co., Ltd., China (Cat. No. P875232). RIF and MOX were purchased from Shandong Sparkjade Biotechnology Co., Ltd. The Cell Counting Kit-8 (CCK-8, 500 assays, C0038, Beyotime Biotechnology, Shanghai, China) and alkaline phosphatase (ALP, 100 assays, P0321S, Beyotime Biotechnology, Shanghai, China) kit were purchased from Beyotime Biotechnology, Shanghai, China. Other reagents used in the experiments were purchased from Sigma without purification.

2.2 Microsphere Preparation

Blank PLGA microspheres and rifampicin (SJ-MA0141, lot no. V1-1-005FMQTU, Shandong Sparkjade Biotechnology Co., Ltd., Jinan, Shandong, China)/moxifloxacin (SJ-MA0386, lot no. M2-2-029WDGMF, Shandong Sparkjade Biotechnology Co., Ltd., Jinan, Shandong, China)-loaded PLGA microspheres were prepared according to our previously reported method. Briefly, 240 mg PLGA and 30 mg Rifampin were dissolved in dichloromethane (DCM) as the oil phase (o). 1 mL of 30 mg/mL moxifloxacin solution was taken as the inner aqueous phase and mixed into the oil phase with stirring to obtain a uniform primary emulsion (w/o). Continuous stirring was maintained while 40 mL of 1% PVA solution was added to obtain a double emulsion (w/o/w), followed by the addition of 800 mL of 0.5% PVA and continued stirring for 10 hours. The prepared microspheres were collected at the bottom of the container. The microspheres were lyophilized for 24 h before use.

2.3 Cell Preparation and Viability Assay

RAW264.7 murine monocyte/macrophage cells were obtained from Zishan Biotechnology Co., Ltd. (Wuhan, China; cat. no. STCC20020). According to the supplier's datasheet, RAW264.7 cells are mouse-derived monocyte/macrophage cells with irregular morphology and adherent growth. Cell line identity was confirmed by the supplier-provided STR authentication report, which showed a 95.20% match with RAW264.7 in Cellosaurus/CLASTR. All cell lines were validated by STR profiling and tested negative for mycoplasma. Cells were maintained in DMEM-H supplemented with 10% fetal bovine serum (FBS) at 37 °C in a humidified incubator with 5% CO_2. During passaging, trypsin was not used; cells were detached by gentle pipetting or with a cell scraper according to the supplier's instructions. Then, mouse macrophages were seeded in a 96-well plate (5×10^5 cells/well) and cultured for 24 hours. Subsequently, the medium was replaced with medium containing different concentrations of RIF/MOX-PLGA microspheres (1 mg/mL, 4 mg/mL, 8 mg/mL, 12 mg/mL) and cultured for an additional 24 hours. Then, 10 μL of CCK-8 reagent was added to each well, and the cells were further incubated in a 37 °C incubator for 2 hours. The 96-well plate was then placed in a microplate reader (Multiskan FC, Thermo Fisher Scientific, Waltham, MA, USA), and the absorbance was measured at 450 nm according to the manufacturer's instructions. Based on the CCK-8 assay, a cytocompatible working concentration of RIF/MOX-PLGA microspheres for subsequent *in vitro* macrophage experiments was selected. This *in vitro* concentration was used only for cell-culture experiments and was not used as a direct basis for calculating the *in vivo* implanted microsphere mass.

2.4 In Vitro Experiments

2.4.1 Cell Infection and ELISA Assay

RAW264.7 cells in good condition/in the logarithmic growth phase were seeded in a 96-well plate at a density of 5×10^5 cells/mL and cultured in an incubator at 37 °C with 5% CO_2. When the cells reached approximately 50% confluence, the old medium was replaced with 100 μL of medium without FBS for serum starvation for 12 hours. A control group and a microsphere group were established. Each well was inoculated with 20 μL of a 1×10^6 CFU/mL bacterial suspension. After 30 minutes of infection, the bacterial suspension was discarded, and the cells were washed three times with pre-warmed sterile PBS at 37°C. The microsphere group was then cultured in medium containing RIF/MOX-PLGA microspheres at 4 mg/mL for 24 hours, whereas the infected control group received an equal volume of microsphere-free medium. After treatment, the cell culture supernatants were collected. The levels of interleukin (IL)-6, IL-1β, and IL-10 in the macrophage supernatant were detected strictly according to the kit instructions.

2.4.2 Cell Immunofluorescence Staining

Three wells each from the microsphere group and the control group were selected for CD38 and CD206 immunofluorescence staining. The culture medium was removed using a pipette, and the cells were washed three times with PBS solution. Then, the cells were fixed with 4% paraformaldehyde (500 mL, P0099-500 mL, Beyotime Biotechnology, Shanghai, China) at room temperature for 20 minutes. The cells were permeabilized with 0.4% Triton X-100 solution for 10 minutes. After washing three times with PBS, The cells were incubated with anti-CD38 and anti-CD206 antibodies overnight at room temperature. The cells were washed three times with PBS, then DAPI solution was added and incubated for 20 minutes at room temperature. After washing with PBS, images were captured using an inverted fluorescence microscope. CD38 was used here as a marker associated with pro-inflammatory macrophage activation, although it is not specific to M1 macrophages; additional markers such as iNOS and CD86 are required for definitive classification.

2.4.3 Protein Assay

The expression levels of PTGS2, YTHDC1, and PDPK1 proteins were quantitatively analyzed by Western blot, with β-actin serving as the internal reference control. The treated Raw264.7 cells were lysed, and protein concentration was determined using the BCA method. First, protein samples were separated by SDS-PAGE gel electrophoresis, and the separated proteins were transferred onto a PVDF membrane. Subsequently, the membrane was blocked to reduce non-specific binding. The membrane was then incubated with primary antibodies against for PTGS2, YTHDC1, PDPK1, and the internal reference antibody β-

actin. After incubation, the membrane was washed and developed using ECL chromogenic reagent. Finally, quantitative analysis of the developed bands was performed using ImageJ image analysis software (version 1.54k, National Institutes of Health, Bethesda, MD, USA), and the experimental data were normalized to the expression level of β-actin.

2.5 In Vivo Experiments

2.5.1 Bacterial Culture

Methicillin-resistant Staphylococcus aureus (MRSA; ATCC 43300; cat. no. B80950; Ningbo Mingzhou Biotechnology Co., Ltd., Ningbo, Zhejiang, China) was inoculated onto agar plates and cultured at 37 °C for 24 hours. After inoculation, a bacterial suspension containing 1.2×10^7 CFU/mL was prepared for subsequent use.

2.5.2 Establishment of a Traumatic Osteomyelitis Animal Model

The animal experiments were reviewed and approved by the Medical Research Ethics Review Committee of the General Hospital of Ningxia Medical University (approval no. KYLL-2022-0731). All surgical procedures were conducted in accordance with the regulations of the Ethics Committee. The animal procedures were also performed in accordance with the Guide for the Care and Use of Laboratory Animals (8th edition; National Research Council, 2011). Fifty-four male SPF mice (provided by the Animal Experiment Center of Ningxia Medical University; 4 weeks old; body weight, approximately 20 g) were randomly divided into three groups: the control group, model group, and microsphere treatment group, with 18 mice in each group.

To ensure animal welfare, a rigorous monitoring and pain management protocol was implemented. In addition to isoflurane anesthesia during surgery, mice received subcutaneous injections of meloxicam (5 mg/kg) postoperatively and once daily for the following three days to provide analgesia. The clinical status of each mouse, including mobility, food and water consumption, and wound healing or infection signs, was monitored once daily by trained personnel. Humane endpoints were established as weight loss exceeding 20% of baseline, persistent inability to eat or drink, or severe, spreading wound suppuration. In this study, all 54 mice (18 per group) successfully tolerated the FRI induction and treatment procedures, surviving until their scheduled observation time points (7, 14, or 28 days). No animals reached the humane endpoints, and none were euthanized early due to excessive suffering.

Before surgery, animals were anesthetized with isoflurane (3% for induction and 1.5%–2% for maintenance, R510-22, RWD Life Science Co., Ltd., Shenzhen, Guangdong, China). Mice were anesthetized with 3% isoflurane for induction and maintained under 1.5–2% isoflurane in oxygen during surgery. After anesthesia, the limbs were immobilized, and the right lower limb was shaved and disinfected. A 5 mm incision was made on the dorsal side of the femur to expose the bone surface. A 25-gauge needle was used to drill a hole through the cortical bone at the midshaft of the femur. A sterile stainless steel needle with a diameter of 0.3 mm was inserted into the medullary cavity through the hole. The model group received an injection of 2 μL of a 1×10^6 CFU/mL Staphylococcus aureus suspension into the medullary cavity using a microsyringe. The control group received an injection of the same volume of sterile PBS after drilling. The microsphere treatment group received an injection of an equal amount of *S. aureus* suspension, followed by the placement of 8 mg of microspheres. The *in vivo* dose was selected as a fixed local implant mass rather than being converted from the *in vitro* CCK-8 concentration. The 4 mg/mL concentration obtained from the CCK-8 assay represented a cytocompatible working concentration for macrophage culture, whereas the 8 mg dose represented the total mass of microspheres locally implanted into the femoral defect to serve as a depot formulation. Therefore, these two values reflect different experimental systems and are not directly interchangeable. The skin was closed, and postoperative disinfection was performed.

2.5.3 Imaging Examination

On postoperative days 7, 14, and 28, experimental mice were randomly selected from the three groups to observe signs including incision redness, swelling, healing, abscess formation, and sinus tract formation. X-ray examination was performed to assess bone resorption, bone destruction, and new bone formation. Scoring was conducted according to the Rissing scoring criteria to evaluate the therapeutic effect after intervention.

2.5.4 Western Blot Detection of Protein Expression

On postoperative day 14, bone tissue from the modeling area was thoroughly scraped and placed in a mortar containing liquid nitrogen to grind the bone tissue into powder. Total protein was extracted from the bone tissue using protein extraction buffer. Western blot was performed to detect the expression levels of YTHDC1, PDPK1, and PTGS2.

2.5.5 Measurement of Inflammatory Factors in Serum

On postoperative days 7, 14, and 28, experimental mice were randomly selected for the detection of TNF-α, IL-6, IL-1β, and IL-10. Blood was collected from the mice via enucleation and centrifuged at 3000 rpm for 10 minutes at 4 °C to collect serum samples. The levels of TNF-α, IL-6, IL-1β, and IL-10 in the serum were measured using ELISA kits (purchased from Beijing Solarbio Science & Technology Co., Ltd.). All operations were strictly performed according to the kit instructions. First, serum samples and standards were added to a 96-well plate pre-coated with antibodies. Then, biotin-labeled antibod-

ies were added. After incubation and washing, horseradish peroxidase-labeled avidin was added, followed by another incubation and washing step. Finally, a chromogenic substrate was added. Qualitative or quantitative analysis was performed based on the intensity of the color reaction. Absorbance (OD value) was measured at a wavelength of 450 nm using a microplate reader, and the concentrations of the inflammatory factors were calculated using a standard curve.

2.5.6 Histopathological Examination

The mice were deeply anesthetized via intraperitoneal injection of an excessive dose of pentobarbital sodium (150 mg/kg, 50 mg/mL, P3761, Sigma-Aldrich, St. Louis, MO, USA). After complete loss of consciousness and reflexes, cervical dislocation was used as an auxiliary physical method to confirm death. The cessation of heartbeat and respiration was verified to ensure that the animals were euthanized. Bone tissue from the femoral lesion area was collected. The tissue was first fixed in 4% paraformaldehyde and then decalcified with 10% EDTA for 6 weeks. Subsequently, the tissue was dehydrated using an ethanol gradient. The dehydrated tissue was embedded in paraffin, sectioned, and finally stained. Hematoxylin and eosin (HE) staining was used to observe bone infection.

2.5.7 Immunofluorescence Staining of Histopathological Sections

Fixed, decalcified, and sectioned bone tissue samples were subjected to immunofluorescence staining for CD38 and CD206. First, the sections were placed on glass slides and incubated with specific antibodies against CD38 and CD206 [anti-CD38 antibody (rabbit monoclonal, clone E9F5A; 1:100-1:400; Cat. No. 68336; Cell Signaling Technology, Danvers, MA, USA) and anti-CD206/MRC1 antibody (rabbit monoclonal, clone E6T5J; 1:200-1:800; Cat. No. 24595; Cell Signaling Technology, Danvers, MA, USA)] to allow the antibodies to bind to the CD38 and CD206 proteins in the sections. The sections were washed to remove unbound antibodies. Fluorescently labeled secondary antibodies [anti-rabbit IgG (H+L), $F(ab')_2$ fragment secondary antibody conjugated to Alexa Fluor 488 (goat; 1:500-1:2000; Cat. No. 4412; Cell Signaling Technology, Danvers, MA, USA) and goat anti-rabbit IgG Fc fragment secondary antibody conjugated to Alexa Fluor 594 (1:2000 for paraffin-embedded sections; Cat. No. 70872; Cell Signaling Technology, Danvers, MA, USA)] were used to incubate the sections, allowing the secondary antibodies to bind to the already bound specific antibodies, thus forming an antigen-antibody-fluorescently labeled secondary antibody complex. The sections were washed again to remove unbound fluorescently labeled secondary antibodies. A fluorescence microscope was used to observe the expression and distribution of CD38 and CD206 proteins in the lesion bone tissue.

2.5.8 HE Staining of Internal Organs.

The heart, lung, kidney, liver, and spleen tissues were collected, and perform H&E staining to assess the potential toxicity of RM-PLGA *in vivo*.

2.6 Statistical Analysis

Statistical analysis was performed using IBM SPSS 25.0 software (version 25.0, IBM Corp., Armonk, NY, USA). Quantitative data are presented as mean ± standard deviation (SD) ($n \geq 3$). For multiple-group comparisons, one-way ANOVA followed by post hoc tests should be used. A p-value < 0.05 was considered statistically significant. All *in vitro* experiments were independently repeated three times. Technical replicate measurements within each experiment were averaged, and the resulting mean was treated as one biological replicate for statistical analysis.

3. Results

3.1 Phenotypic Changes of Macrophages in In Vitro Experiments

Rifampicin/moxifloxacin-loaded PLGA microspheres were successfully prepared according to previous methods. *In vitro*, the CCK-8 assay showed that 4 mg/mL was a cytocompatible working concentration for RAW264.7 macrophages among the tested concentrations (Fig. 1A). Therefore, 4 mg/mL was selected for subsequent *in vitro* macrophage experiments. This concentration was not used as a direct basis for determining the *in vivo* implanted microsphere mass. After infecting macrophages with *S. aureus*, for 30 minutes, the cells were washed and then treated with RM-PLGA microspheres (4 mg/mL) or control medium for 24 hours. Compared with the control group, the levels of IL-6 and IL-1β factors (Fig. 1B,C) were significantly reduced in the microsphere treatment group, while the level of IL-10 was significantly increased (Fig. 1D). These findings suggest that RM-PLGA treatment was associated with decreased pro-inflammatory cytokine levels and increased IL-10 levels under infected conditions. However, these results do not distinguish whether the observed changes resulted from direct macrophage modulation or from reduced bacterial burden and subsequent inflammatory resolution. Cell immunofluorescence staining was further used to assess CD38 and CD206 expression. Compared with the control group, the RM-PLGA group showed significantly lower fluorescence intensities of both CD38 and CD206 (Fig. 1E,F). Together with the cytokine findings, these results suggest that RM-PLGA treatment was associated with changes in macrophage polarization-related marker expression and the inflammatory microenvironment under infected conditions.

3.2 Expression of YTHDC1 and PDPK1 in Macrophages in In Vitro Experiments

The results indicated that the expression levels of YTHDC1 and PDPK1 in the control group were higher than

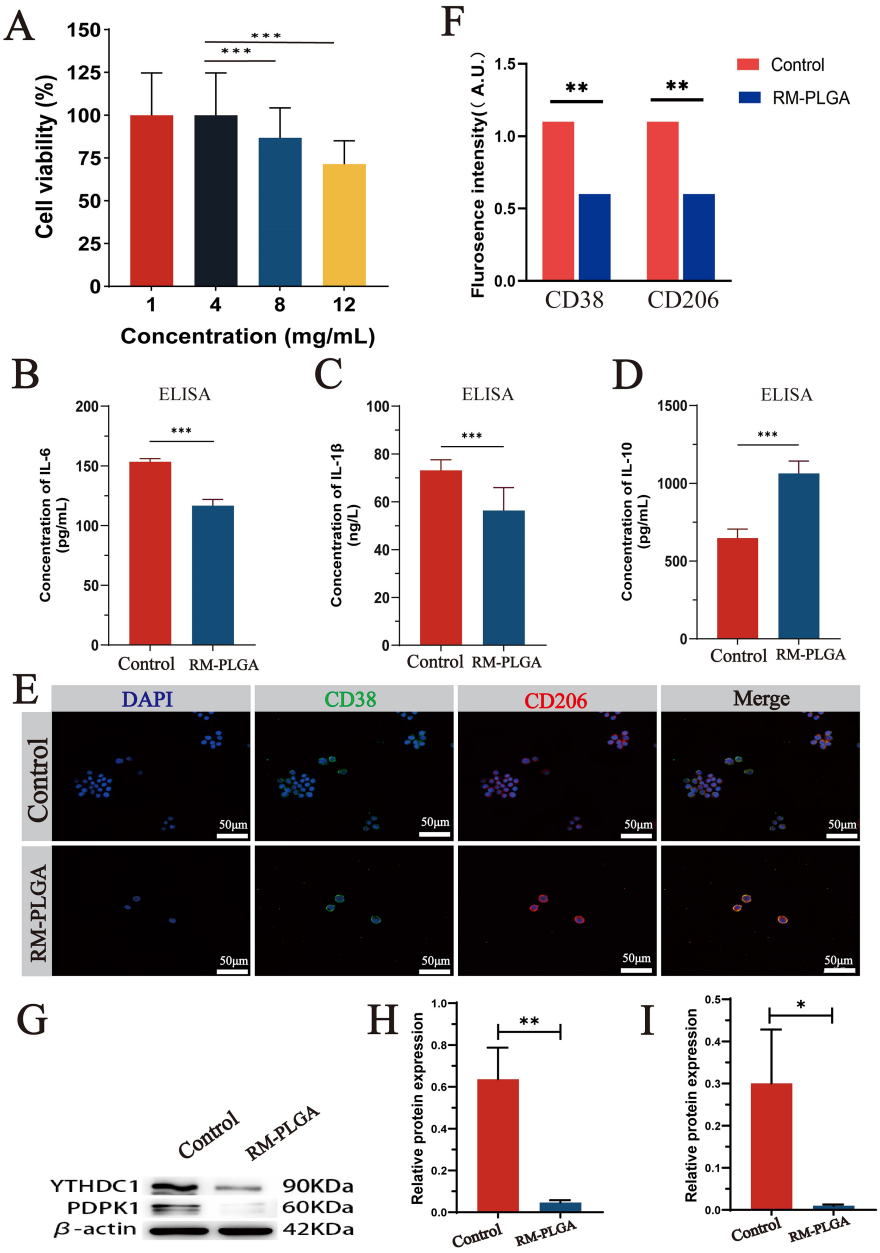

Fig. 1. Effects of RM-PLGA microspheres on macrophage viability, inflammatory cytokines, polarization-associated markers, and YTHDC1/PDPK1 expression *in vitro*. (A) The CCK-8 results of co-culture of the four concentrations of RIF/MOX-PLGA microspheres (1, 4, 8, and 12 mg/mL) with macrophages. (B) ELISA results for IL-6. (C) It represents the ELISA results of the IL-1β factor. (D) It represents the ELISA results of the IL-10 factor. (E) Cellular immunofluorescence staining of CD38 and CD206. Scale bar = 50 μm. (F) Quantification of CD38 and CD206 fluorescence intensities. (G) Immunoblotting detection of two proteins in macrophages. (H) Quantitative analysis of YTHDC1 protein. (I) Quantitative analysis of PDPK1 protein. Abbreviations: PLGA, poly(lactic-co-glycolic acid) copolymer; RM, rifampicin–moxifloxacin; CCK-8, Cell Counting Kit-8; ELISA, enzyme-linked immunosorbent assay; IL, interleukin; YTHDC1, YTH domain-containing protein 1; PDPK1, 3-phosphoinositide-dependent protein kinase 1. In panel (A), comparisons were made between 4 mg/mL and 8 or 12 mg/mL, as indicated by the brackets. In panels (B–D,F,H,I), comparisons were made between the S. aureus-infected control group without microspheres and the S. aureus-infected RM-PLGA group treated with 4 mg/mL microspheres. $*p < 0.05$, $**p < 0.01$, $***p < 0.001$; Data are presented as mean ± SD from three independent experiments (n = 3 biological replicates). Technical replicate wells within each experiment were averaged before statistical analysis.

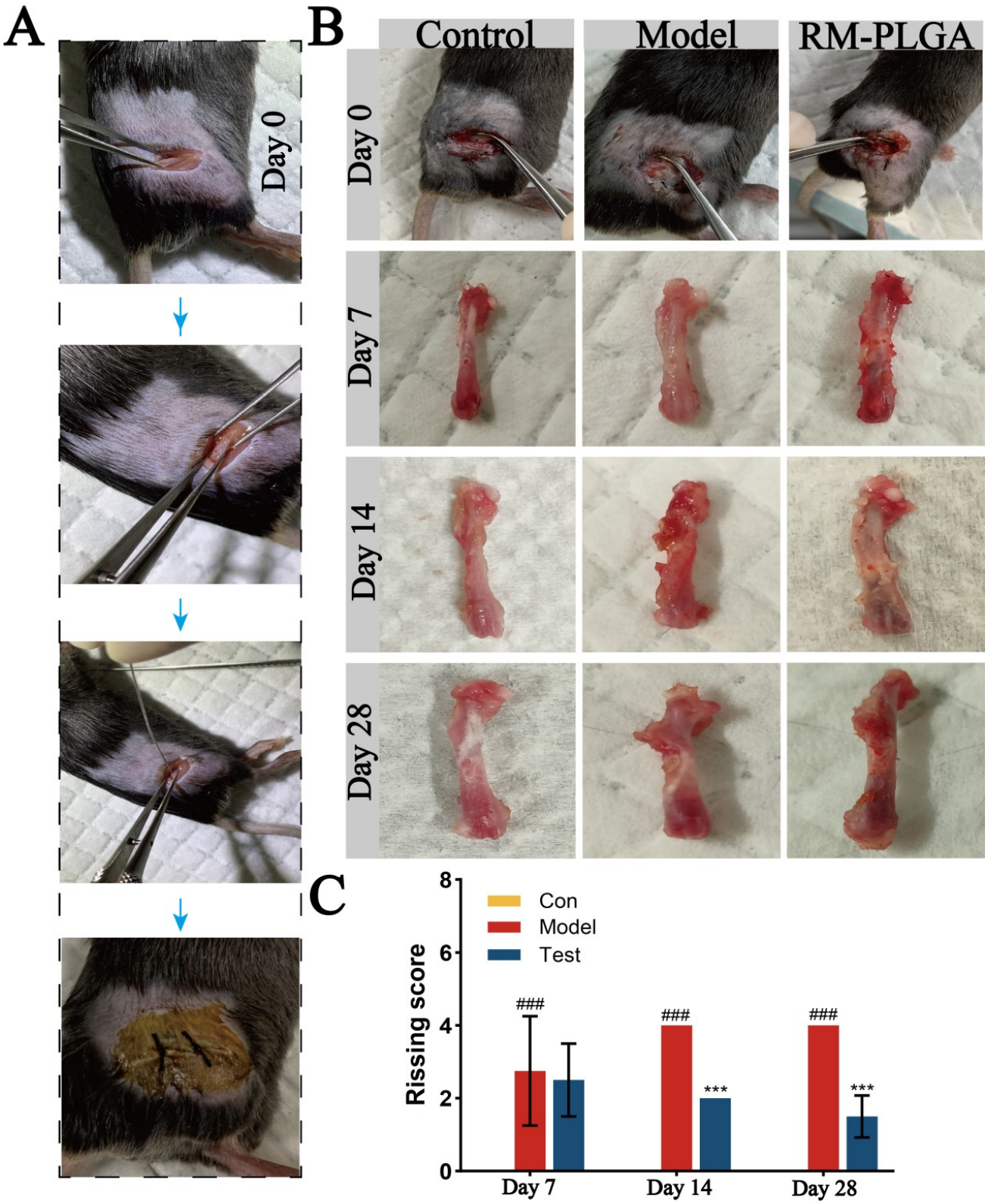

Fig. 2. Establishment and gross evaluation of the mouse femoral osteomyelitis model. (A) Flowchart for establishing an infectious osteomyelitis model in mice. (B) Growth of the modeling area in the control group, model group, and microsphere group at days 0, 7, 14, and 28. (C) Rissing scores of the control group, model group, and microsphere group. Abbreviations: PLGA, poly(lactic-co-glycolic acid) copolymer; RM, rifampicin–moxifloxacin. ###$p < 0.001$ versus the control group; ***$p < 0.001$ versus the model group; n = 3.

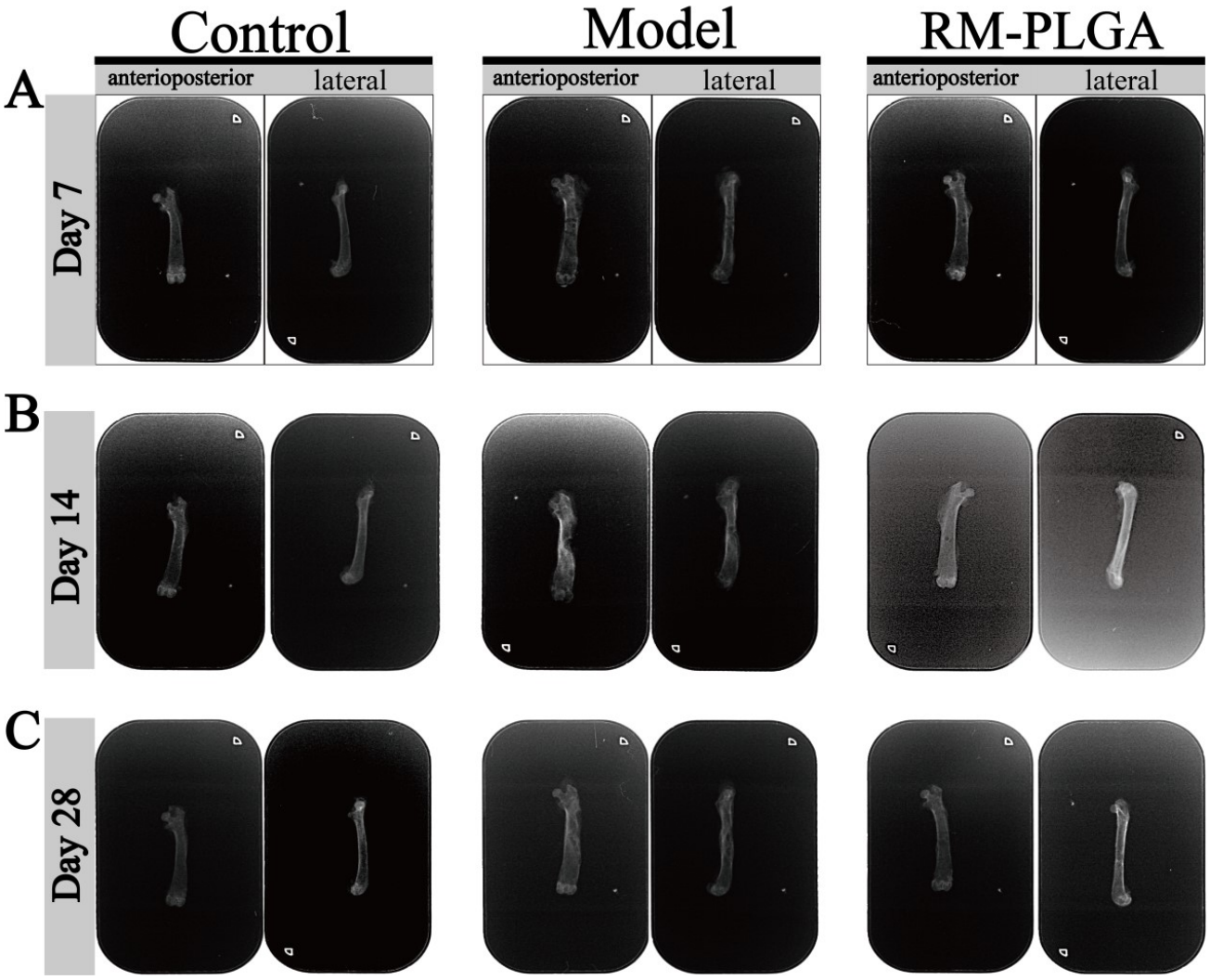

Fig. 3. X-ray examination results, including frontal and lateral films. (A) X-ray conditions of the control group, model group and microsphere group on the 7th day after surgery. (B) X-ray conditions on the 14th day after surgery. (C) X-ray conditions on the 28th day after surgery. Abbreviations: PLGA, poly(lactic-co-glycolic acid) copolymer; RM, rifampicin–moxifloxacin.

those in the microsphere group (Fig. 1G–I). *In vitro* Western blot analysis showed that YTHDC1 and PDPK1 expression levels differed between the control and microsphere-treated groups (Fig. 1G–I). These results indicate that YTHDC1 and PDPK1 expression was reduced in RM-PLGA-treated infected RAW264.7 macrophages. Because RAW264.7 cells are macrophages and do not represent osteoblasts or other bone-resident cells, these *in vitro* findings should be interpreted as macrophage-specific expression changes under infected conditions. However, because no pathway inhibition, knockdown, overexpression, or rescue experiments were performed, the present data cannot determine whether YTHDC1 or PDPK1 directly mediates the macrophage polarization induced by RM-PLGA. Therefore, these results should be interpreted as preliminary expression-level evidence.PTGS2 expression was not clearly detected under the present *in vitro* conditions, which may be related to the timing of detection or the transient nature of PTGS2 expression. Further time-course experiments are needed to clarify this issue.

3.3 In Vivo Experiments

3.3.1 Gross Appearance Observations

All mice survived the surgical procedure (Fig. 2A). Gross observations of the animals were conducted at 7, 14, and 28 days (Fig. 2B) and assessed using the Rissing score (Fig. 2C). In the control group animals, the wounds showed no significant redness, swelling, or exudation and tended to heal. The model group exhibited significant redness and swelling, with some experimental mice developing pus discharge, and sinus tracts gradually formed at the wound sites. Animals in the microsphere treatment group showed no wound redness, swelling, or exudation, and the wounds had largely healed by day 14. In the mouse femora/femoral specimens, the model group had purulent secretions within the needle tracts, with the diameter gradually increasing.

The microsphere treatment group showed no significant purulent secretions, and the needle tract diameter did not expand.

3.3.2 Imaging Findings

X-ray examinations were performed on the surgical sites of the mice at 7, 14, and 28 days postoperatively to observe the presence of subperiosteal abscesses, bone destruction, and sequestrum formation. At 7 days, the control group and the microsphere group showed the presence of Kirschner wire bone channels, with no formation of subperiosteal abscesses. In the model group, periosteal thickening and subperiosteal abscess formation were observed (Fig. 3A). At 14 days, the control group and the microsphere group still showed no abscess formation, with the bone channels gradually showing signs of healing. In the model group, the extent of abscess formation in the lesion area increased, with partial bone sclerosis(Fig. 3B). At 28 days, the bone channels in both the control group and the microsphere group had healed, with no sequestrum formation. In contrast, the model group exhibited bone destruction, sequestrum formation, and showed typical radiographic features of chronic osteomyelitis(Fig. 3C).

3.3.3 Western Blot Detection of Protein Expression Results

On day 14, the microsphere group showed the highest YTHDC1 expression, followed by the control group, while the model group had the lowest expression. On day 14, Western blot analysis showed that YTHDC1 and PDPK1 expression levels were higher in the microsphere treatment group than in the model group, whereas PTGS2 showed the opposite trend (Fig. 4A–D). These expression changes were consistent with reduced inflammation and improved tissue repair observed in the microsphere group. However, the current results only indicate an association between RM-PLGA treatment and changes in YTHDC1, PDPK1, and PTGS2 expression. Further functional experiments are required to determine whether these molecules directly regulate macrophage polarization or bone repair in this model. In contrast to the *in vitro* macrophage model, *in vivo* bone tissue samples showed higher YTHDC1 and PDPK1 expression in the RM-PLGA group. This difference may reflect the complexity of the *in vivo* osteomyelitis microenvironment, which contains multiple cell populations and dynamic inflammatory-repair processes (Fig. 4A,B). PDPK1 expression followed the same trend as YTHDC1 (Fig. 4C), while PTGS2 showed the opposite pattern (Fig. 4D). PTGS2 is an inflammation-related enzyme that has been implicated in bone inflammatory responses. In the present study, PTGS2 expression was lower in the RM-PLGA group than in the model group, which may reflect attenuation of infection-associated inflammatory stimulation. However, because bacterial burden and PTGS2 pathway activity were not directly quantified, this finding should be interpreted as an association rather than evidence of a direct causal mechanism.

3.3.4 Changes in Inflammatory Factors In Vivo

Serum levels of tumor necrosis factor-α (TNF-α), IL-6, IL-1β, and IL-10 in experimental animals were measured on days 7, 14, and 28 (Fig. 4E–H). Compared to the control group, serum levels of TNF-α, IL-6, and IL-1β were significantly elevated at all three time points (day 7, day 14, and day 28) ($p < 0.001$). However, intervention with microspheres significantly reduced serum levels of TNF-α, IL-6, and IL-1β ($p < 0.001$), indicating that microspheres significantly suppressed the inflammatory response in osteomyelitis and promote its recovery. Compared to the control group, serum IL-10 levels were significantly elevated at all three time points (day 7, day 14, and day 28) ($p < 0.05$, $p < 0.01$, $p < 0.001$). Compared to the model group, serum IL-10 levels were significantly reduced at 7d ($p < 0.01$), showed no significant change at 14d ($p > 0.05$), and were significantly reduced at 28d ($p < 0.001$).

3.3.5 Histopathological Manifestations

Animals were randomly selected from the control group, model group, and microsphere group and euthanized at 7, 14, and 28 days of the experiment, respectively. Lesion area tissues were collected for HE staining (Fig. 5). The control group showed normal cortical bone structure and osteocytes within the medullary cavity. In the model group, infiltration by lymphocytes and plasma cells was observed on day 7, which gradually increased by day 14. By day 28, in addition to lymphocytes and plasma cells, sequestrum formation and some reactive new bone were visible. Compared to the model group, the microsphere group showed a small number of lymphocytes and plasma cells, with no sequestrum formation observed.

3.3.6 Expression of CD206 and CD38 in Pathological Tissues

Immunofluorescence staining and fluorescence quantification were performed to evaluate CD38 and CD206 expression in pathological tissues at days 7, 14, and 28 (Fig. 6A–D). In the control group, CD38-positive and CD206-positive cells were detected at low levels at the three time points, indicating a mild local response after traumatic intervention. In the model group, CD38 expression showed an overall decreasing trend from day 7 to day 28, whereas CD206 expression increased over the same period, indicating distinct temporal changes in macrophage polarization-associated markers in the lesion area. In the microsphere group, CD38 expression was lower than that in the model group, whereas CD206 expression showed a relatively higher reparative marker profile during treatment progression.

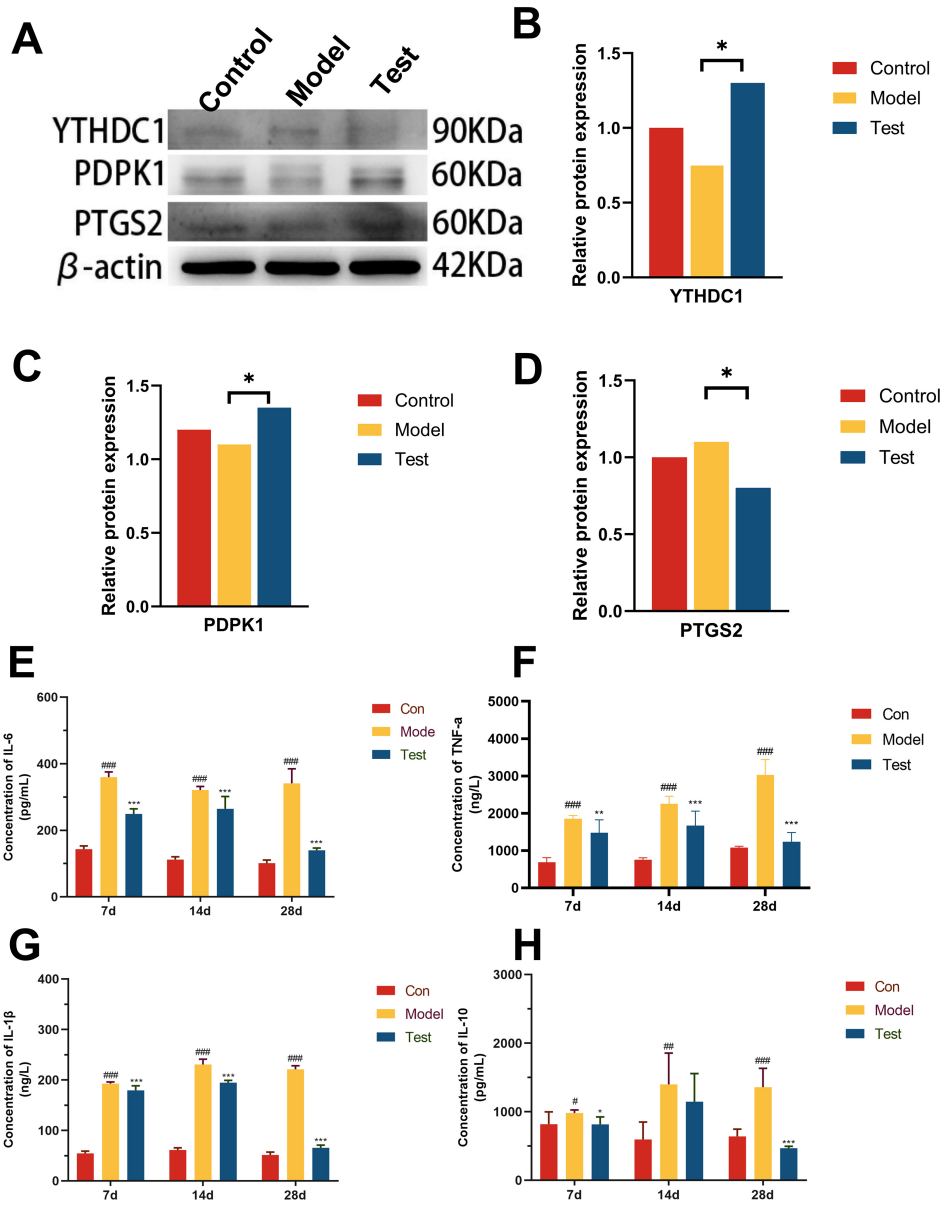

Fig. 4. Effects of RM-PLGA treatment on YTHDC1, PDPK1, and PTGS2 expression and serum inflammatory cytokines *in vivo*. (A) Western blotting was performed to detect the protein expression levels of YTHDC1, PDPK1, and PTGS2 on the 14th day. (B) Quantification of YTHDC1 protein expression. (C) Quantitative analysis of the protein of PDPK1. (D) Quantitative analysis of the protein of PTGS2. (E) Level of IL-6 in serum. (F) Level of TNF-α in serum. (G) Level of IL-1β in serum. (H) Level of IL-10 in serum. Abbreviations: PLGA, poly(lactic-co-glycolic acid) copolymer; RM, rifampicin–moxifloxacin. In all panels, the control group is shown in red, the model group in yellow, and the RM-PLGA treatment group in blue. "Con" denotes the control group, and "Test" denotes the RM-PLGA treatment group. For panels (B–D), $*p < 0.05$ for the indicated pairwise comparisons. For panels (E–H), $\#p < 0.05$, $\#\#p < 0.01$, and $\#\#\#p < 0.001$ versus the control group at the corresponding time point; $*p < 0.05$, $**p < 0.01$, and $***p < 0.001$ versus the model group at the corresponding time point; n = 3.

3.3.7 Results of HE Staining of Internal Organs

The results (Fig. 7) show that the morphology of various tissues is intact. Compared with the control group, there are no obvious signs of organ damage in the experimental group, suggesting that RM-PLGA did not cause obvious organ toxicity.

4. Discussion

As the most challenging and highly prevalent complication in the field of orthopedics, the treatment of traumatic osteomyelitis always faces multiple challenges. The core pathological features of this disease are concentrated in the formation of bacterial biofilms, progressive destruc-

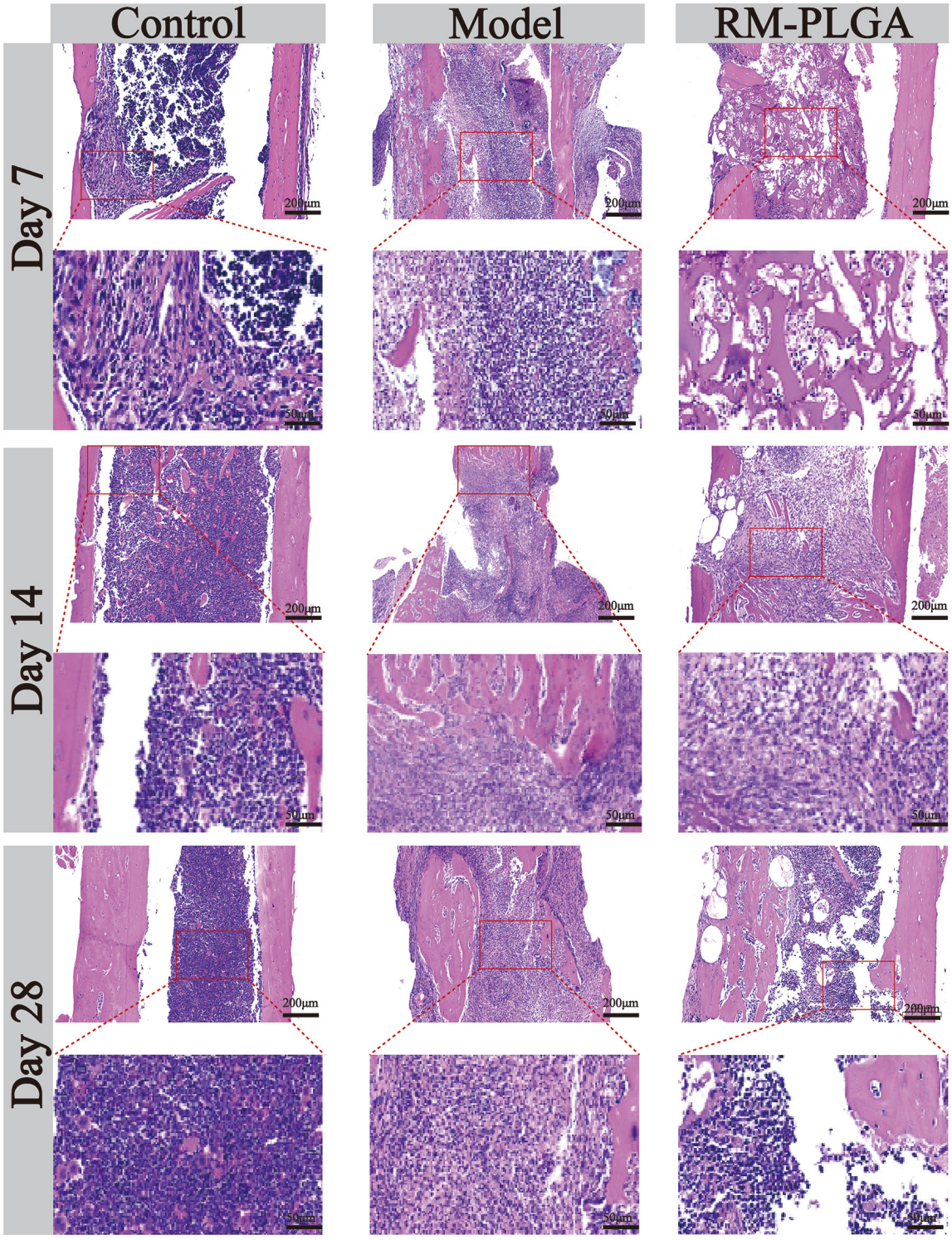

Fig. 5. The results of HE staining of the modeling area on the 7th, 14th and 28th days after the operation. PLGA, poly(lactic-co-glycolic acid) copolymer; RM, rifampicin–moxifloxacin; HE, Hematoxylin and eosin. Scale bars = 200 μm in the upper panels and 50 μm in the magnified lower panels.

tion of bone tissue, and dysregulation of the host immune microenvironment [14]. These three factors intertwine to form a vicious cycle, making it difficult for traditional treatment plans to achieve a cure. Through systematic *in vitro* and *in vivo* validation, this study showed that rifampicin/moxifloxacin-loaded PLGA microspheres effectively alleviated infection-related pathological changes in a traumatic osteomyelitis model and were accompanied by changes in macrophage polarization markers. However, because the present study did not include antibiotic-

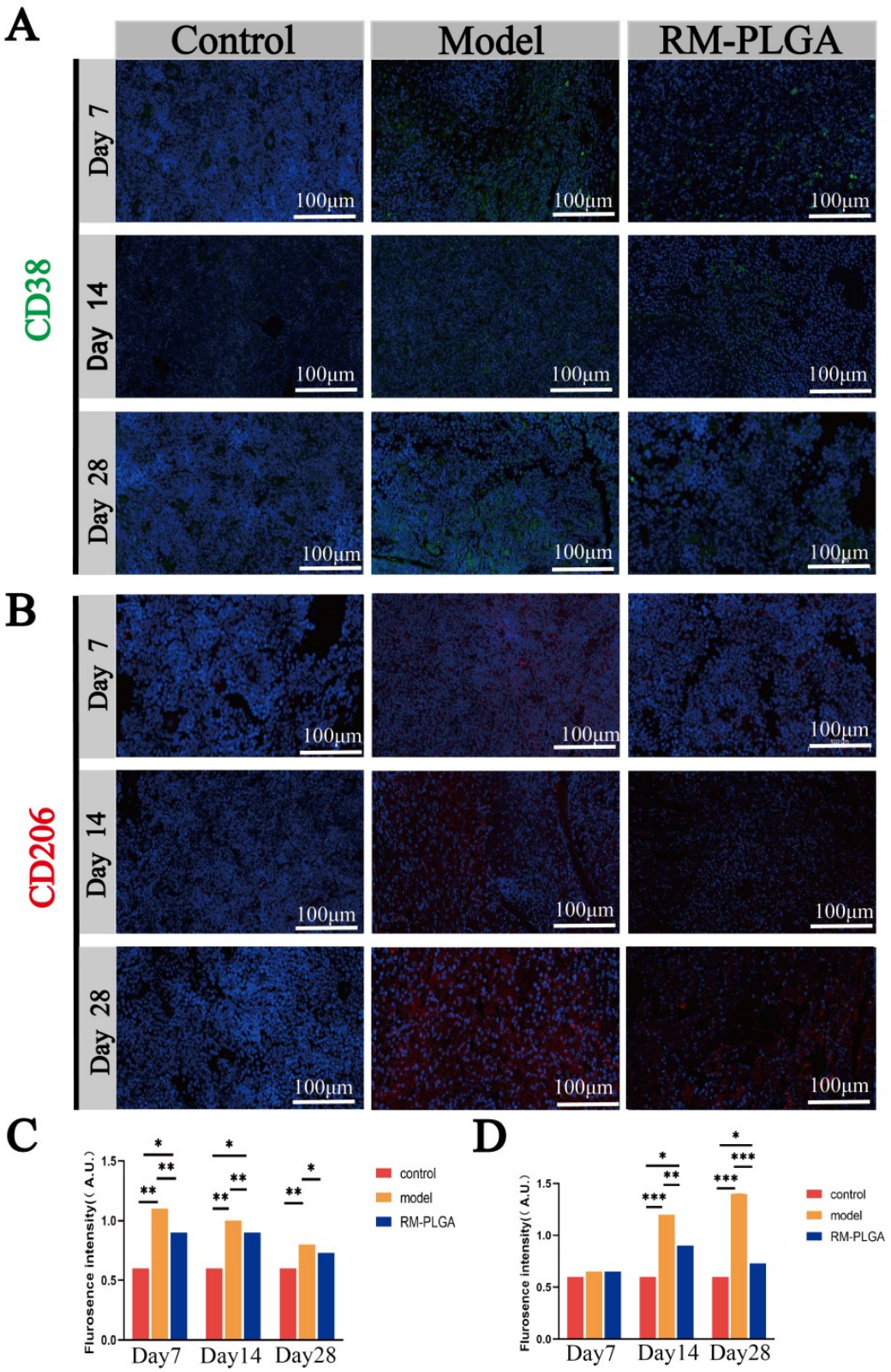

Fig. 6. The number of cells was detected on the 7th, 14th, and 28th days using the cell immunofluorescence staining method. (A) CD38-positive cells. Scale bar = 100 μm. (B) CD206-positive cells. Scale bar = 100 μm. (C) Quantification of CD38-positive cells. (D) Quantification of CD206-positive cells. Abbreviations: PLGA, poly(lactic-co-glycolic acid) copolymer; RM, rifampicin-moxifloxacin. *$p < 0.05$, **$p < 0.01$, ***$p < 0.001$; n = 3.

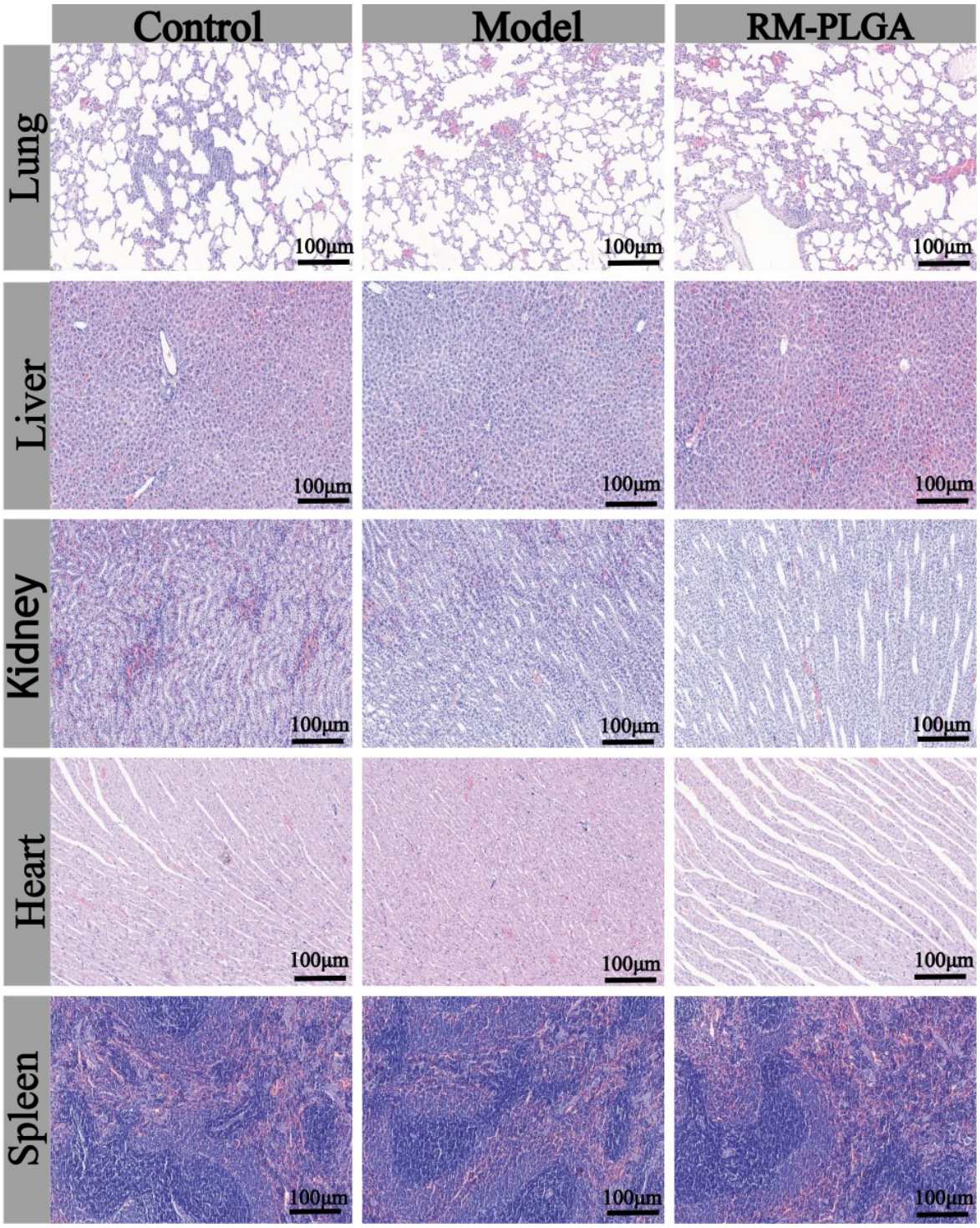

Fig. 7. HE staining of the heart, lungs, kidneys, liver and spleen of mice. PLGA, poly(lactic-co-glycolic acid) copolymer; RM, rifampicin-moxifloxacin. Scale bar = 100 μm.

only or blank microsphere plus antibiotic control groups, the observed macrophage polarization changes should be interpreted as treatment-associated immunological alterations rather than definitive evidence of an independent immunomodulatory activity of the microspheres [32]. RM-PLGA treatment was associated with a decrease in pro-inflammatory markers and a relative changes in CD206/IL-10-associated reparative markers, which may reflect remodeling of the inflammatory microenvironment during infection control and tissue repair [33,34].

The RM-PLGA microspheres used in this study were designed as a local antibiotic delivery system for rifampicin and moxifloxacin. Our previous *in vitro* study demonstrated that RIF/MOX-PLGA microspheres exhibited sus-

tained drug-release behavior, antibacterial activity, and biofilm-inhibition effects against *S. aureus*. In the present *in vivo* osteomyelitis model, RM-PLGA treatment alleviated wound swelling, abscess formation, bone destruction, inflammatory cytokine elevation, and histopathological injury. These findings are consistent with a therapeutic effect of locally implanted RM-PLGA microspheres.

However, the present study did not directly measure rifampicin or moxifloxacin concentrations in lesion bone tissue, surrounding soft tissue, or serum after implantation. Therefore, it cannot be concluded from the current data that the microspheres maintained local antibiotic concentrations above the MIC for MRSA over time. The observed therapeutic efficacy should be attributed to RM-PLGA treatment as a whole, rather than definitively ascribed to a verified *in vivo* sustained-release pharmacokinetic profile. Future studies should use HPLC or LC-MS/MS to quantify rifampicin and moxifloxacin concentrations at the infection site and in serum at multiple time points, and compare these concentrations with the MIC values of the infecting MRSA strain.

Based on our previous *in vitro* findings, RM-PLGA microspheres showed sustained-release behavior and antibiofilm activity against *S. aureus*. In the present *in vivo* study, the improved pathological outcomes may be related to local antibacterial effects of RM-PLGA treatment; however, direct *in vivo* evidence for continuous drug exposure and biofilm disruption was not obtained. In terms of drug synergy, rifampin has unique bactericidal activity against intracellular bacteria and biofilm-associated bacteria, while moxifloxacin, as a broad-spectrum fluoroquinolone, exhibits strong antibacterial effects against both aerobic and anaerobic bacteria. The combination of rifampicin and moxifloxacin significantly reduced the risk of drug resistance, indicating a synergistic antibacterial effect between the two antibiotics. In addition, the carrier properties of PLGA microspheres may prolong local antibiotic exposure at the infection site, thereby further enhancing the antibacterial efficacy of the combined drugs, although this still requires confirmation through *in vivo* pharmacokinetic analysis. These findings are highly consistent with the experimental results, including significantly reduced inflammatory factors IL-6 and IL-1β in the microsphere group *in vitro*, as well as the absence of purulent secretions and sequestrum formation in the lesion area *in vivo*.

An important finding of this study is that RM-PLGA treatment was associated with changes in macrophage polarization markers. The reduction of pro-inflammatory cytokines and CD38-positive cells, together with changes in CD206 and IL-10, suggests that RM-PLGA may help remodel the inflammatory microenvironment in traumatic osteomyelitis. As the core effector cells of innate immunity, macrophages play a dual role in inflammatory responses and tissue repair: classically activated M1 macrophages are induced by interferon-γ (IFN-γ) or lipopolysaccharide (LPS), and express high levels of pro-inflammatory factors such as TNF-α, IL-1β, and IL-6, with the main function of clearing pathogens. However, excessive and sustained activation of M1 macrophages can lead to severe tissue damage and impair the bone repair process. In contrast, alternatively activated M2 macrophages are induced by IL-4 and IL-13 and play important roles in anti-inflammatory regulation, tissue repair, and bone regeneration, etc., highly expressing anti-inflammatory factors such as IL-10 and TGF-β, as well as arginase-1 (Arg-1), with the core role of suppressing excessive inflammation, clearing apoptotic cells, promoting angiogenesis, and tissue remodeling. CD38 expression can also be induced in other cell types and under non-M1 conditions; therefore, this limitation should be considered when interpreting the immunofluorescence data.

It should be noted that the observed changes in IL-10 and CD206 and the decrease in pro-inflammatory cytokines and CD38 may represent a natural consequence of effective bacterial clearance and resolution of acute inflammation. Because the present study did not include antibiotic-only, blank PLGA microsphere, or blank PLGA plus free-antibiotic control groups, we cannot determine whether the macrophage polarization-associated changes were directly induced by the microsphere material, by rifampicin/moxifloxacin, or indirectly caused by reduced bacterial burden. Therefore, these data should be interpreted as treatment-associated immunological alterations accompanying infection control, rather than definitive evidence of an independent immunomodulatory activity of RM-PLGA.

In the pathological process of traumatic osteomyelitis, persistent stimulation by pathogens and their toxins can maintain a sustained pro-inflammatory macrophage-associated state, thereby contributing to chronic inflammation and impaired bone repair. Therefore, a shift from a sustained pro-inflammatory macrophage profile toward a reparative macrophage-associated profile is considered beneficial for resolving inflammation and supporting bone repair. The results of this study support an association between RM-PLGA treatment and changes in macrophage polarization-related markers. *In vitro*, RM-PLGA treatment reduced IL-6 and IL-1β levels and increased IL-10 levels after bacterial infection. Immunofluorescence staining showed significantly lower fluorescence intensities of both CD38 and CD206 in the RM-PLGA group than in the control group. *In vivo*, RM-PLGA treatment was also associated with reduced inflammatory injury and changes in macrophage polarization markers. Immunofluorescence staining showed reduced CD38-positive signals in the RM-PLGA group, whereas CD206-positive signals were comparable to those in the model group on day 7 and were lower on days 14 and 28. These findings indicate changes in macrophage polarization-associated marker expression in the lesion area, but they do not by themselves establish functional macrophage reprogramming. Pathological ex-

amination showed reduced inflammatory tissue injury and no obvious sequestrum formation in the RM-PLGA group. Together with the macrophage marker findings, these results suggest that RM-PLGA treatment was associated with improvement of the local inflammatory microenvironment, which may provide favorable conditions for bone repair.

5. Limitations

This study has several limitations. First, the mechanistic investigation remains preliminary. Although RM-PLGA treatment was accompanied by changes in YTHDC1, PDPK1, and PTGS2 expression, the present study did not include functional validation experiments, such as YTHDC1 or PDPK1 knockdown/overexpression, PTGS2 inhibition, pathway blockade, or rescue assays. Second, macrophage polarization analysis in this study was primarily based on immunofluorescence staining of CD38 and CD206, combined with inflammatory cytokine detection. Although these results consistently indicated that RM-PLGA treatment was associated with favorable changes in macrophage polarization-associated marker expression, the marker panel used remained relatively limited. Incorporating additional classical M1/M2 markers, such as iNOS, CD86, Arg-1, and CD163, as well as flow cytometry analysis, would provide more comprehensive and quantitative evidence for macrophage polarization. Future studies will include a broader panel of macrophage markers and flow cytometry to further validate the immunomodulatory effects of RM-PLGA. Therefore, the current data cannot establish a direct causal relationship between these molecules and RM-PLGA-induced macrophage polarization. Third, the potential signaling pathway was inferred mainly from protein expression changes and phenotypic markers. Future studies should use loss- and gain-of-function approaches, pathway inhibitors, mRNA-level validation, and rescue experiments to determine whether YTHDC1, PDPK1, and PTGS2 are necessary and/or sufficient for RM-PLGA-associated macrophage polarization changes.

Another limitation of the present study is that the antibacterial efficacy was mainly evaluated indirectly through gross observation, imaging findings, histopathological changes, and inflammatory cytokine levels. Although these results consistently indicated that RM-PLGA treatment alleviated infection-related pathological changes *in vivo*, direct quantitative bacterial analyses, such as CFU counting, bacterial load determination, and *in vivo* biofilm-related assays, were not performed in the current study. In our previous work, the same RIF/MOX–PLGA microspheres were shown to possess direct *in vitro* antibacterial and antibiofilm activities, including stronger bacterial killing, larger inhibition zones, and significant inhibition of both early and mature *S. aureus* biofilms [31]. Therefore, the present study focused primarily on *in vivo* therapeutic efficacy and macrophage polarization. Future studies will incorporate CFU counting, bacterial burden quantification, and biofilm evaluation to further confirm the direct antibacterial efficacy of RM-PLGA *in vivo*.

Another limitation is that the *in vivo* dose of RM-PLGA microspheres was not optimized through a dose-ranging experiment. In the present study, the 4 mg/mL concentration identified by the CCK-8 assay was used only as a cytocompatible working concentration for *in vitro* macrophage experiments. This concentration cannot be directly converted into the 8 mg local implant dose used in the mouse femoral defect model, because the former represents microsphere mass per culture-medium volume, whereas the latter represents the total mass of microspheres implanted locally as a depot formulation. Therefore, although the present data demonstrate therapeutic efficacy at the selected 8 mg dose, they do not define the minimally effective dose, optimal dose, or dose-response relationship of RM-PLGA microspheres *in vivo*. Future studies should include multiple *in vivo* doses to clarify the dose-response profile and optimize the local implantation dose.

In addition, the present study lacked *in vivo* pharmacokinetic analysis of rifampicin and moxifloxacin after local implantation of RM-PLGA microspheres. Although our previous *in vitro* study demonstrated sustained drug release and antibacterial activity of RIF/MOX-PLGA microspheres, the present study did not measure rifampicin or moxifloxacin concentrations in lesion bone tissue, surrounding soft tissue, or serum. Therefore, the current data cannot directly confirm whether local antibiotic concentrations remained above the MIC for MRSA over time. This limitation restricts the ability to attribute the observed therapeutic efficacy specifically to the intended sustained-release drug-delivery function. Future studies should quantify local and systemic rifampicin/moxifloxacin concentrations using HPLC or LC-MS/MS at multiple post-implantation time points and compare these concentrations with the MIC of the infecting MRSA strain.

A further limitation of this study is that the current experimental design cannot fully distinguish the direct immunomodulatory effect of RM-PLGA microspheres from the secondary immunological changes caused by bacterial clearance. The study did not include several critical control groups, such as systemic rifampicin/moxifloxacin at equivalent effective doses, blank PLGA microspheres combined with systemic antibiotics, or locally delivered free rifampicin/moxifloxacin. Therefore, the observed decrease in pro-inflammatory cytokines and CD38-positive cells, together with changes in CD206/IL-10-associated reparative markers in the microsphere group, may be partly or largely attributable to infection control and subsequent resolution of inflammation. The present findings should therefore be interpreted as showing that RM-PLGA treatment was associated with macrophage polarization-related changes in the infected microenvironment, rather than proving an independent macrophage-polarizing property of the microspheres. Future studies incorporating these control groups will be

necessary to clarify the relative contributions of antibacterial activity, local sustained drug release, PLGA carrier effects, and direct macrophage immunomodulation.

Notably, YTHDC1 and PDPK1 showed opposite trends between the *in vitro* RAW264.7 macrophage model and the *in vivo* osteomyelitis model. This discrepancy may be explained by the different biological contexts of the two systems. The *in vitro* experiments were performed exclusively in macrophages, whereas the *in vivo* bone lesion tissue contained macrophages, osteoblast-lineage cells, stromal cells, endothelial cells, and infiltrating immune cells. Therefore, the increased YTHDC1 and PDPK1 expression observed *in vivo* cannot be attributed specifically to macrophages based on the current data. These findings should be interpreted as tissue-level expression changes associated with infection resolution and repair, rather than direct evidence of macrophage-specific regulation.

6. Conclusion

In summary, the present study demonstrates that rifampicin/moxifloxacin-loaded PLGA microspheres alleviated infection-related pathological changes and reduced inflammatory responses in a traumatic osteomyelitis model. RM-PLGA treatment was associated with favorable changes in macrophage polarization-associated markers, including reduced pro-inflammatory cytokines and CD38-positive cells together with changes in CD206/IL-10-associated reparative markers. Together with our previous *in vitro* findings showing sustained antibiotic release, direct antibacterial activity, and biofilm inhibition of RIF/MOX–PLGA microspheres [31], these results suggest that RM-PLGA microspheres may serve as a promising local therapeutic strategy for traumatic osteomyelitis. However, antibiotic-only, blank PLGA plus antibiotic, and locally delivered free antibiotic control groups were not included in the present study. Therefore, it remains unclear whether the observed macrophage polarization-associated changes were caused by a direct immunomodulatory effect of RM-PLGA or were secondary to bacterial clearance and inflammation resolution. Further studies incorporating these control groups, as well as CFU counting, bacterial burden quantification, and *in vivo* biofilm-related assays, are required to clarify the relative contributions of antibacterial activity and macrophage immunomodulation and to directly confirm the antibacterial efficacy of RM-PLGA *in vivo*.

Availability of Data and Materials

The datasets generated and analyzed during the current study are available from the corresponding author on reasonable request.

Author Contributions

JA and YZ contributed to conceptualization, data curation, formal analysis, investigation, methodology, software, visualization, writing—original draft, and writing—review and editing. PZ and DT contributed to methodology and supervision. HS, ZY, and HG contributed to supervision and validation. YW and HF contributed to data curation and investigation. ZQ contributed to conceptualization, funding acquisition, resources, supervision, validation, writing—original draft, and writing—review and editing. All authors contributed to editorial revisions of the manuscript. All authors have read and approved the final manuscript. All authors have participated sufficiently in the work and agree to be accountable for all aspects of the work.

Ethics Approval and Consent to Participate

The animal experiments were reviewed and approved by the Medical Research Ethics Review Committee Ethics Committee of the General Hospital of Ningxia Medical University (approval no. KYLL-2022-0731). All surgical procedures were conducted in accordance with the regulations of the Ethics Committee. The animal procedures were also performed in accordance with the Guide for the Care and Use of Laboratory Animals (8th edition; National Research Council, 2011) and the ARRIVE guidelines.

Acknowledgment

We would like to express our sincere gratitude to all those who provided support and assistance during the preparation of this manuscript. We also thank the reviewers for their valuable comments and suggestions.

Funding

This work was supported by the National Natural Science Foundation of China (Grant No. 82460431) and the Natural Science Foundation of Ningxia Province (Grant No. 2023AAC02064).

Conflicts of Interest

The authors declare no conflicts of interest.

Supplementary Material

Supplementary material associated with this article can be found, in the online version, at https://doi.org/10.31083/FBL52014.

References

[1] Wang X, Yu S, Sun D, Fu J, Wang S, Huang K, et al. Current data on extremities chronic osteomyelitis in southwest China: epidemiology, microbiology and therapeutic consequences. Scientific Reports. 2017; 7: 16251. https://doi.org/10.1038/s41598-017-16337-x

[2] Zhang H, Qiao W, Liu Y, Yao X, Zhai Y, Du L. Addressing the challenges of infectious bone defects: a review of recent advances in bifunctional biomaterials. Journal of

Nanobiotechnology. 2025; 23: 257. https://doi.org/10.1186/s12951-025-03295-0

[3] Li J, Jiang B, Yang L, Zhang P, Wu J, Yang Y, et al. Dual-functional titanium implants via polydopamine-mediated lithium and copper co-incorporation: synergistic enhancement of osseointegration and antibacterial efficacy. Frontiers in Bioengineering and Biotechnology. 2025; 13: 1593545. https://doi.org/10.3389/fbioe.2025.1593545

[4] Ji B, Zhang L, Xiao L, Guo Z, Liu Z. Antibacterial Agent-Loaded Hydrogels for Implant-Associated Osteomyelitis: A Review. Macromolecular Bioscience. 2026; 26: e00528. https://doi.org/10.1002/mabi.202500528

[5] Li Z, He D, Guo B, Wang Z, Yu H, Wang Y, et al. Self-promoted electroactive biomimetic mineralized scaffolds for bacteria-infected bone regeneration. Nature Communications. 2023; 14: 6963. https://doi.org/10.1038/s41467-023-42598-4

[6] Panteli M, Giannoudis PV. Chronic osteomyelitis: what the surgeon needs to know. EFORT Open Reviews. 2016; 1: 128–135. https://doi.org/10.1302/2058-5241.1.000017

[7] Conterno LO, Turchi MD. Antibiotics for treating chronic osteomyelitis in adults. The Cochrane Database of Systematic Reviews. 2013; 2013: CD004439. https://doi.org/10.1002/14651858.CD004439.pub3

[8] Haidar R, Der Boghossian A, Atiyeh B. Duration of post-surgical antibiotics in chronic osteomyelitis: empiric or evidence-based? International Journal of Infectious Diseases. 2010; 14: e752–e758. https://doi.org/10.1016/j.ijid.2010.01.005

[9] Nandi SK, Bandyopadhyay S, Das P, Samanta I, Mukherjee P, Roy S, et al. Understanding osteomyelitis and its treatment through local drug delivery system. Biotechnology Advances. 2016; 34: 1305–1317. https://doi.org/10.1016/j.biotechadv.2016.09.005

[10] Gomes D, Pereira M, Bettencourt AF. Osteomyelitis: an overview of antimicrobial therapy. Brazilian Journal of Pharmaceutical Sciences. 2013; 49: 13–27.

[11] Li K, Yu S, Lin D, Zhang X, Liang Y, He D, et al. Imaging observation of allogeneic bone and bone-induced calcium phosphate biomaterials as supplements in the treatment of infectious bone defects. Journal of Orthopaedic Surgery (Hong Kong). 2025; 33: 10225536251362765. https://doi.org/10.1177/10225536251362765

[12] Greimel F, Scheuerer C, Gessner A, Simon M, Kalteis T, Grifka J, et al. Efficacy of antibiotic treatment of implant-associated *Staphylococcus aureus* infections with moxifloxacin, flucloxacillin, rifampin, and combination therapy: an animal study. Drug Design, Development and Therapy. 2017; 11: 1729–1736. https://doi.org/10.2147/DDDT.S138888

[13] Spellberg B, Lipsky BA. Systemic antibiotic therapy for chronic osteomyelitis in adults. Clinical Infectious Diseases : an Official Publication of the Infectious Diseases Society of America. 2012; 54: 393–407. https://doi.org/10.1093/cid/cir842

[14] Masters EA, Trombetta RP, de Mesy Bentley KL, Boyce BF, Gill AL, Gill SR, et al. Evolving concepts in bone infection: redefining "biofilm", "acute vs. chronic osteomyelitis", "the immune proteome" and "local antibiotic therapy". Bone Research. 2019; 7: 20. https://doi.org/10.1038/s41413-019-0061-z

[15] Hofstee MI, Muthukrishnan G, Atkins GJ, Riool M, Thompson K, Morgenstern M, et al. Current Concepts of Osteomyelitis: From Pathologic Mechanisms to Advanced Research Methods. The American Journal of Pathology. 2020; 190: 1151–1163. https://doi.org/10.1016/j.ajpath.2020.02.007

[16] Pan G, Wang Z, Zhong Q, Li H, Peng S, Shuai C. Ultrasound-responsive MoS_2@pCu-MOF heterojunction scaffold: Enhancing bacterial membrane permeability, exhibiting efficient antibacterial activity and facilitating bone regeneration. Colloids and Surfaces. B, Biointerfaces. 2025; 254: 114872. https://doi.org/10.1016/j.colsurfb.2025.114872

[17] Zimmerli W, Sendi P. Role of Rifampin against Staphylococcal Biofilm Infections *In Vitro*, in Animal Models, and in Orthopedic-Device-Related Infections. Antimicrobial Agents and Chemotherapy. 2019; 63: e01746–18. https://doi.org/10.1128/AAC.01746-18

[18] Tricou LP, Mouton W, Cara A, Trouillet-Assant S, Bouvard D, Laurent F, et al. Staphylococcus aureus can use an alternative pathway to be internalized by osteoblasts in absence of β1 integrins. Scientific Reports. 2024; 14: 28643. https://doi.org/10.1038/s41598-024-78754-z

[19] Rasigade JP, Trouillet-Assant S, Ferry T, Diep B, Sapin A, Lhoste A, et al. PSMs of hypervirulent Staphylococcus aureus act as intracellular toxins that kill infected osteoblasts. PLoS One. 2013; 8: e63176. https://doi.org/10.1371/journal.pone.0063176

[20] Zelmer AR, Nelson R, Richter K, Atkins GJ. Can intracellular Staphylococcus aureus in osteomyelitis be treated using current antibiotics? A systematic review and narrative synthesis. Bone Research. 2022; 10: 53. https://doi.org/10.1038/s41413-022-00227-8

[21] Masters EA, Ricciardi BF, Bentley KLM, Moriarty TF, Schwarz EM, Muthukrishnan G. Skeletal infections: microbial pathogenesis, immunity and clinical management. Nature Reviews. Microbiology. 2022; 20: 385–400. https://doi.org/10.1038/s41579-022-00686-0 (online ahead of print)

[22] Wassif RK, Elkayal M, Shamma RN, Elkheshen SA. Recent advances in the local antibiotics delivery systems for management of osteomyelitis. Drug Delivery. 2021; 28: 2392–2414. https://doi.org/10.1080/10717544.2021.1998246

[23] Makadia HK, Siegel SJ. Poly Lactic-co-Glycolic Acid (PLGA) as Biodegradable Controlled Drug Delivery Carrier. Polymers. 2011; 3: 1377–1397. https://doi.org/10.3390/polym3031377

[24] Hua Y, Su Y, Zhang H, Liu N, Wang Z, Gao X, et al. Poly(lactic-co-glycolic acid) microsphere production based on quality by design: a review. Drug Delivery. 2021; 28: 1342–1355. https://doi.org/10.1080/10717544.2021.1943056

[25] Tamazawa G, Ito A, Miyai T, Matsuno T, Kitahara K, Sogo Y, et al. Gatifloxacine-loaded PLGA and β-tricalcium phosphate composite for treating osteomyelitis. Dental Materials Journal. 2011; 30: 264–273. https://doi.org/10.4012/dmj.2010-098

[26] Kimishima K, Matsuno T, Makiishi J, Tamazawa G, Sogo Y, Ito A, et al. Effects of gatifloxaine content in gatifloxacine-loaded PLGA and β-tricalcium phosphate composites on efficacy in treating osteomyelitis. Odontology. 2016; 104: 105–113. https://doi.org/10.1007/s10266-014-0187-9

[27] Liu Y, Li X, Liang A. Current research progress of local drug delivery systems based on biodegradable polymers in treating chronic osteomyelitis. Frontiers in Bioengineering and Biotechnology. 2022; 10: 1042128. https://doi.org/10.3389/fbioe.2022.1042128

[28] Guo H, Ren C, Wang C, Xu Y, Ma T, Li D. Chronic osteomyelitis after cephalomedullary nailing for intertrochanteric fractures of the femur: carbon fiber rod bone cement combined with calcium sulfate loaded with antibiotics. Journal of Orthopaedic Surgery and Research. 2025; 20: 971. https://doi.org/10.1186/s13018-025-06381-z

[29] Qiu Z, Yuan H, Li N, Yang X, Hu X, Su F, et al. Bidirectional effects of moxifloxacin on the pro-inflammatory response in lipopolysaccharide-stimulated mouse peritoneal macrophages. Molecular Medicine Reports. 2018; 18: 5399–5408. https://doi.org/10.3892/mmr.2018.9569

[30] Chen Y, Li C, Jia J, Jiang Y, Zhang P, Cheng C, et al. COX-2 inhibition as a therapeutic strategy for bone loss in Staphylococcus aureus osteomyelitis. Molecular Medicine (Cambridge, Mass.). 2025; 31: 177. https://doi.org/10.1186/s10020-025-01202-9

[31] Qiao Z, Yuan Z, Zhang W, Wei D, Hu N. Preparation, in vitro release and antibacterial activity evaluation of rifampicin and moxifloxacin-loaded poly(D,L-lactide-co-glycolide) microspheres. Artificial Cells, Nanomedicine, and Biotechnology. 2019; 47: 790–798. https://doi.org/10.1080/21691401.2019.1581792

[32] Fearing BV, Romereim SM, Danelson K, Smykowski M, Barankevich M, Serbin R, et al. Development of a small animal bone-anchored limb replacement model for infection interventions. OTA International : the Open Access Journal of Orthopaedic Trauma. 2025; 8: e366. https://doi.org/10.1097/OI9.0000000000000366

[33] Hu K, Shang Z, Yang X, Zhang Y, Cao L. Macrophage Polarization and the Regulation of Bone Immunity in Bone Homeostasis. Journal of Inflammation Research. 2023; 16: 3563–3580. https://doi.org/10.2147/JIR.S423819

[34] Zhang R, Tan SF, Wang Y, Wu J, Zhang C. From macrophage polarization to clinical translation: immunomodulatory hydrogels for infection-associated bone regeneration. Frontiers in Cell and Developmental Biology. 2025; 13: 1684357. https://doi.org/10.3389/fcell.2025.1684357